Electronic Supplementary Material (ESI) for Analyst

Electronic Supporting Information (ESI)

A new ditopic ratiometric receptor for detecting zinc and fluoride ions in living cells

Ya-Ping Li,[a] Qiang Zhao,[a] Hua-Rong Yang,[a] Sui-Jun Liu,[a] Xiu-Ming Liu,[a] Ying-Hui Zhang,[a] Tong-Liang Hu,[a] Jia-Tong Chen,[b] Ze Chang,[a,*] and Xian-He Bu[a]

a) Department of Chemistry, TKL of Metal and Molecule-based Material Chemistry; Synergetic Innovation Center of Chemical Science and Engineering (Tianjin), Nankai University, Tianjin 300071, China.

Corresponding author E-mail: buxh@nankai.edu.cn, change@nankai.edu.cn

b) Department of Biochemistry and Molecular Biology, and College of Life Sciences, Nankai University, Tianjin 300071 (China)

The comparison between ESIPT and PET mechanisms

(i) PET mechanism

Upon excitation of the fluorophore, an electron of the highest occupied molecular orbital (HOMO) is promoted to the lowest unoccupied molecular orbital (LUMO), which enables PET (between the frontier obits between cations receptor and fluorophore), and causes fluorescence quenching of the latter (See Scheme S1).

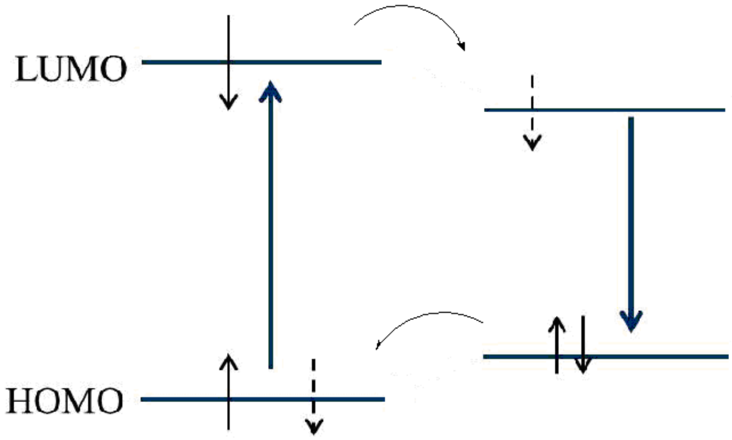

Scheme S1. Principle of cation recognition by fluorescent PET sensor.

(ii) ESIPT mechanism

For example, benzimidazole derivatives (T_A) containing an intramolecular hydrogen bond undergo ESIPT (Scheme S2). The coordination of OH-moieties with Zn^{2+} will remove this proton and disrupt the ESIPT process.

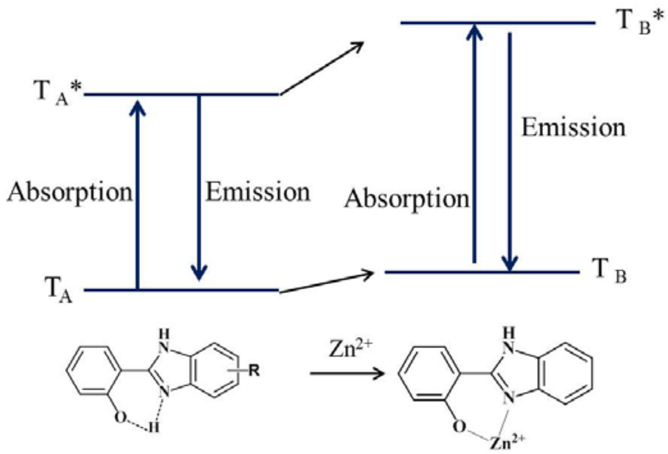

Scheme S2. Simplified Jablonski diagram illustrating the increase of the emission energy upon metal-cation-induced inhibition of ESIPT.

Synthesis of compounds 2 and 3

The dibenzo-18-crown-6 compounds (**2** and **3**) were synthesized according to the literature method.[S1] To a stirring solution of dibenzo-18-crown-6 (6 mmol) in dichloromethane, concentrated nitric acid (15 mL) was added dropwise, and, after 5-10 min, concentrated sulfuric acid (7.5 mL) was added in the same manner. The mixture was stirred at room temperature for 48-72 h. The product (**2**), precipitated out of the solution as a fine yellow powder (yield ~80%), was obtained by filtration, washed with water, and dried in the oven（80 °C）.

2,3,13,14-Tetranitro-6,7,9,10,17,18,20,21-octahydrodibenzo[b,k][1,4,7,10,13,16]hexaoxacyclooctadecine (**2**, 0.50 g) was added to the suspension of Pd/C (0.25 g) in degassed ethanol (50 mL) and hydrazine hydrate (15 mL), and the resultant mixture was refluxed with stirring for about 4 hours under argon atmosphere. After cooling（反应是否加热？多少度？）, the reaction mixture was filtered to afford compound **3** as white needle-like solids (yield ~20%).

Reference

S1. S. A. Duggan, G. Fallon, S. J. Langford, V. L. Laau, J. F. Satchell, M. N. Paddon-Row, *J. Org. Chem*. **2001,** *66*, 4419.

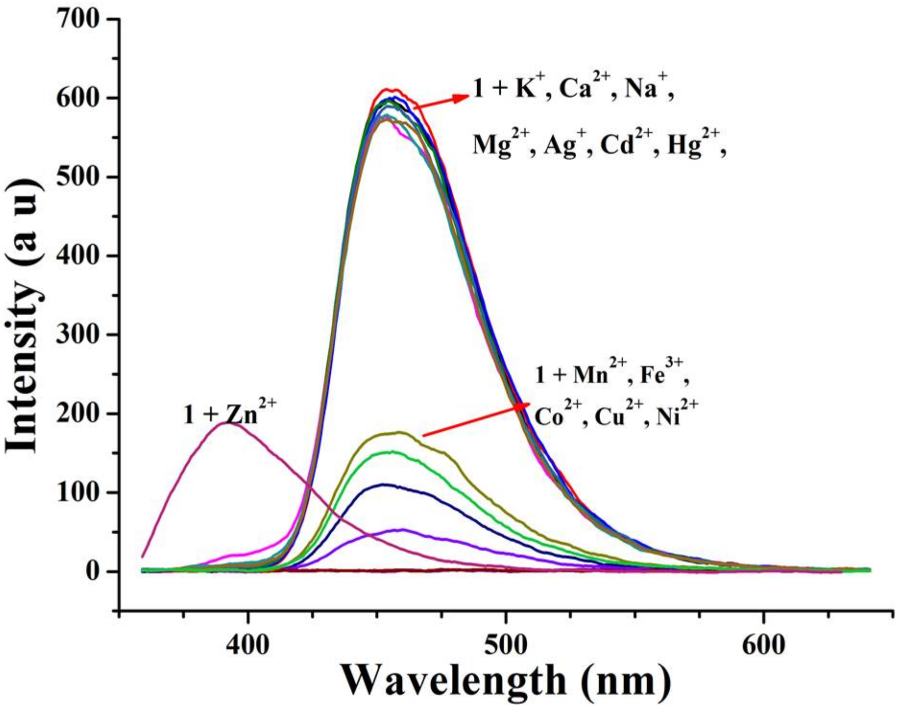

a)

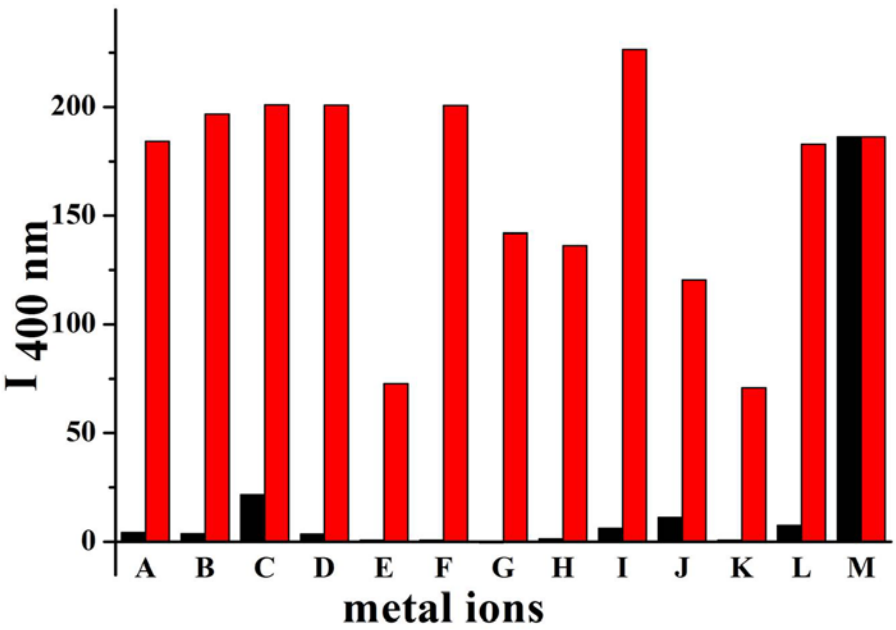

b)

Figure S1. Changes in a) fluorescence spectra of **1** (1.0×10^{-6} M) upon the addition of different cations in CH_3CN solution; b) fluorescence intensity at 400 nm of **1** in the presence of other metal ions in CH_3CN (λ_{ex} = 330 nm); black bars, **1** + competing ions, red bars, **1** + competing ions + Zn^{2+}, (A) K^+, (B) Na^+, (C) Mg^{2+}, (D) Ca^{2+}, (E) Mn^{2+}, (F) Co^{2+}, (G) Cu^{2+}, (H) Ni^{2+}, (I) Cd^{2+}, (J) Hg^{2+}, (K) Fe^{3+}, (L) Ag^+, (M) Zn^{2+}.

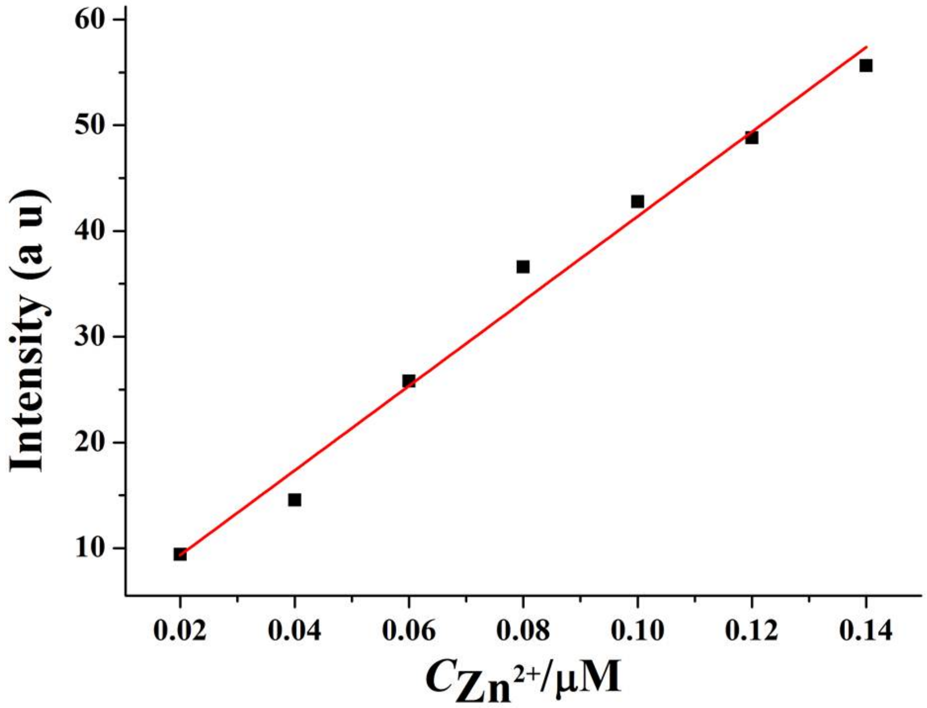

Figure S2. Fluorescence titration of **1** (1.0×10^{-6} M) with $Zn(NO_3)_2$ in CH_3CN. [Zn^{2+}]: 0.02, 0.04, 0.06, 0.08, 0.10, 0.12, 0.14 $\times 10^{-6}$ M.

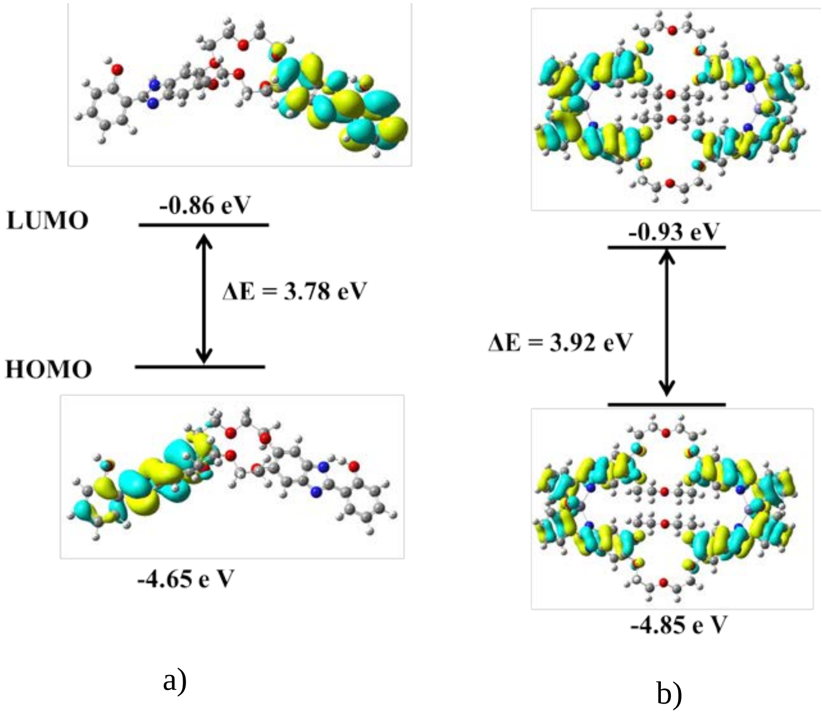

Figure S3. The HOMO–LUMO energy gaps and interfacial plots of the orbitals for: a) free **1**, b) **1**-Zn^{2+} complex, gray, red and blue atoms of the molecular frameworks indicate the C, O, N, and metal atoms, respectively. Gray and cyan deep parts on the interfacial plots refer to the different phases of the molecular wave functions, for which the iso value is 0.02 a.u..

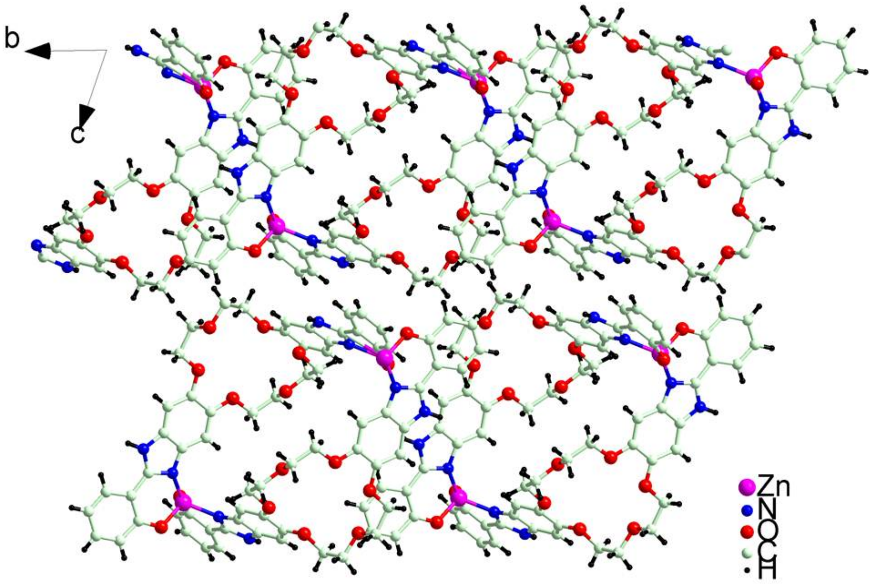

Figure S4. View of the packing diagram of **1**-Zn^{2+} along *a* direction.

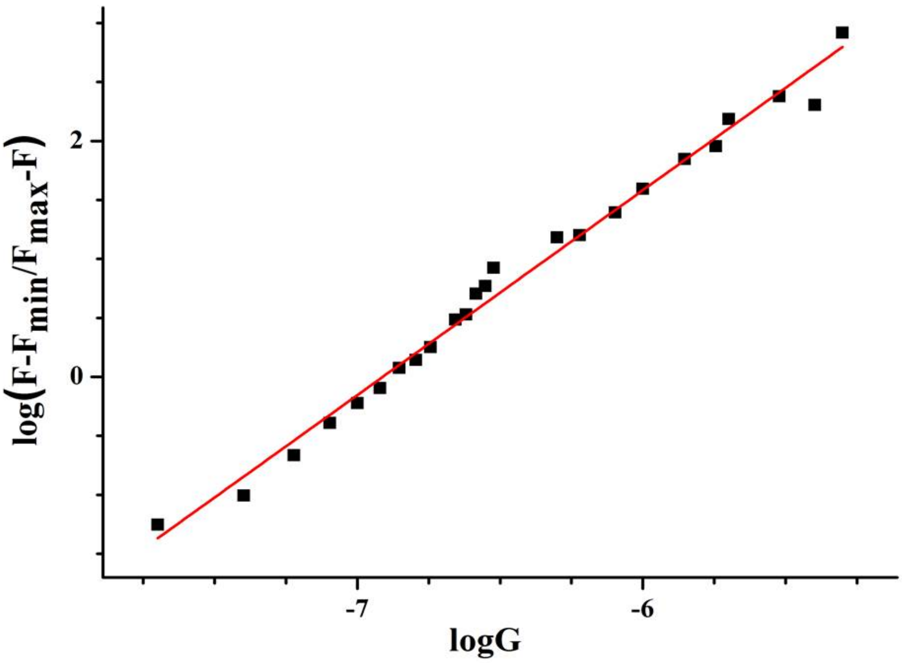

Figure S5. The plot of fluorescence intensity at 400 nm of **1** (1.0×10^{-6} M) *versus* increasing concentration of Zn^{2+} in CH_3CN solution. The excitation and emission slit widths were 2.5 and 5 nm, respectively (λ_{ex} = 330 nm).

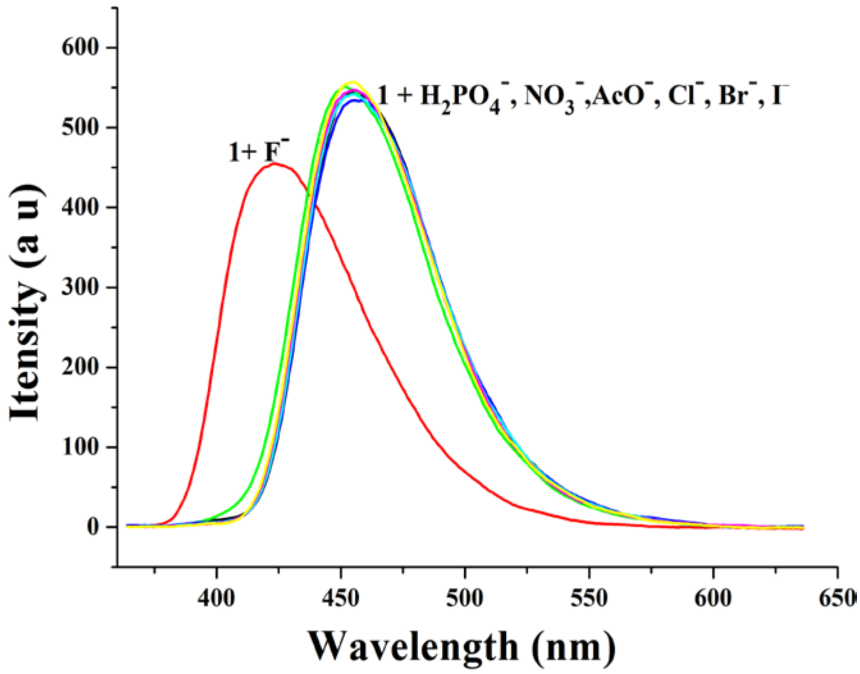

a)

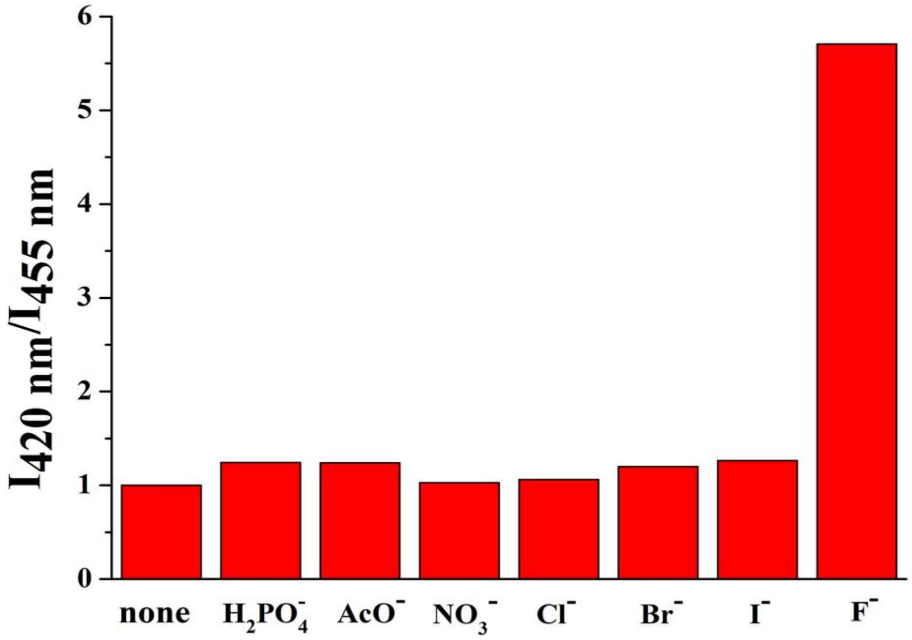

b)

Figure S6. Fluorescent spectral changes of **1** (1.0×10^{-6} M): a) upon addition of different anions (as n-Bu_4N^+ salts) in CH_3CN; b) the intensity changes of **1** upon addition of different anions.

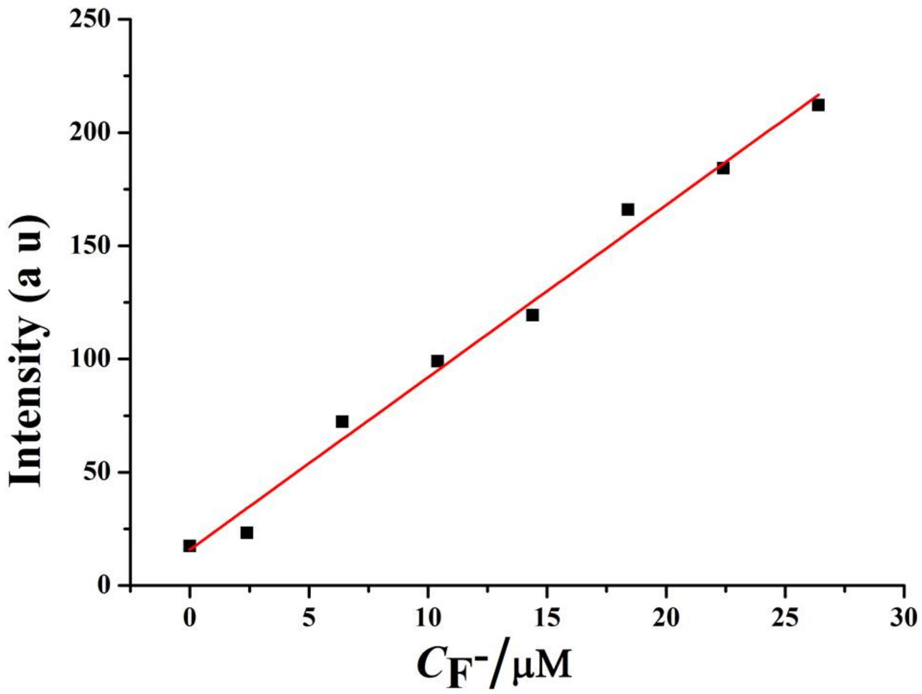

Figure S7. Fluorescence titration of **1** (1.0×10^{-6} M) with TABF in CH_3CN. [F^-]: 0, 2.5, 5,10, 15, 20, 25, 30×10^{-6} M.

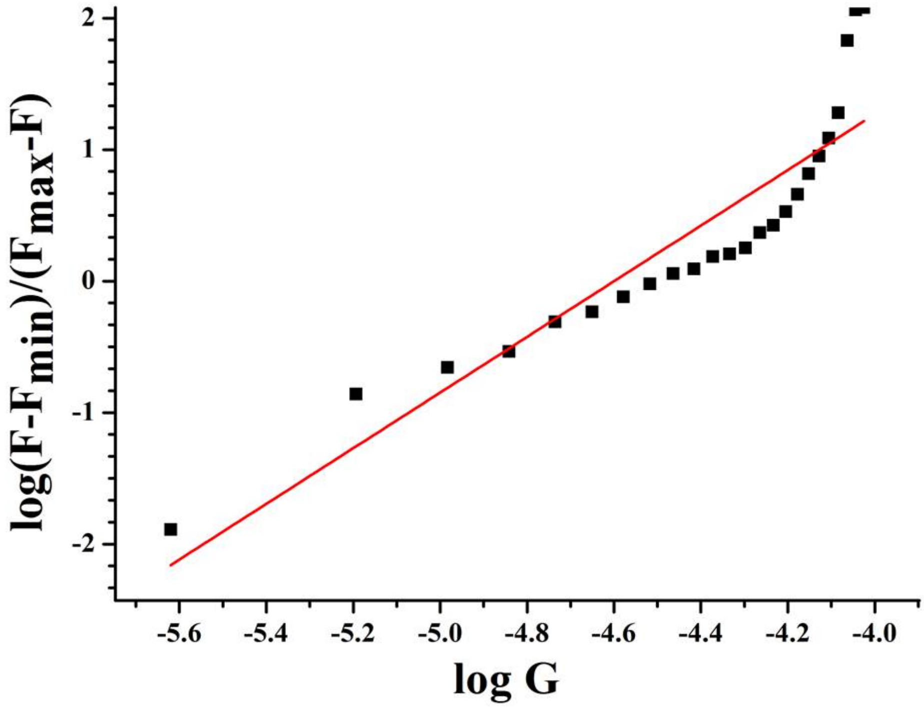

Figure S8. The plot of fluorescence intensity at 420 nm of **1** (1.0 × 10^{-6} M) *versus* increasing concentration of F^{-} in CH_3CN solution. The excitation and emission slit widths were 2.5 and 5 nm, respectively (λ_{ex} = 330 nm).

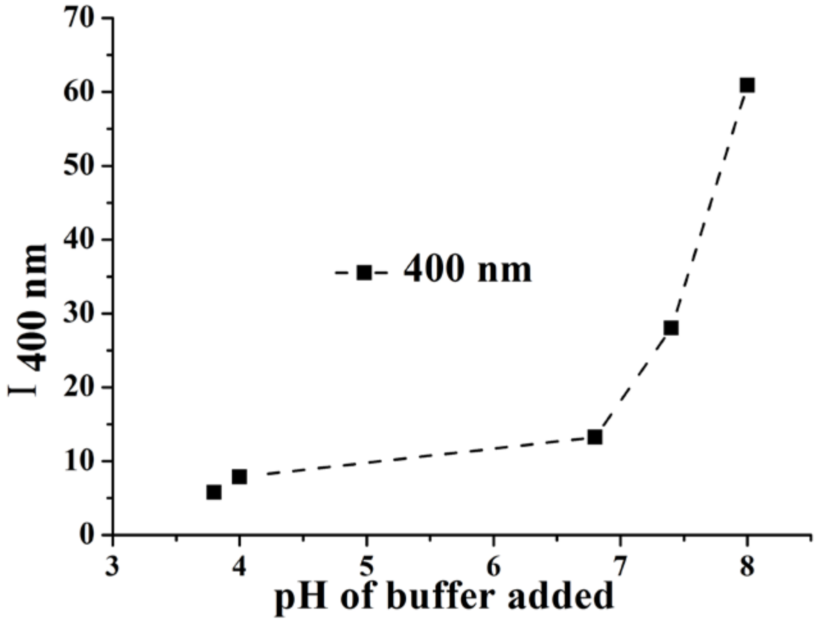

a)

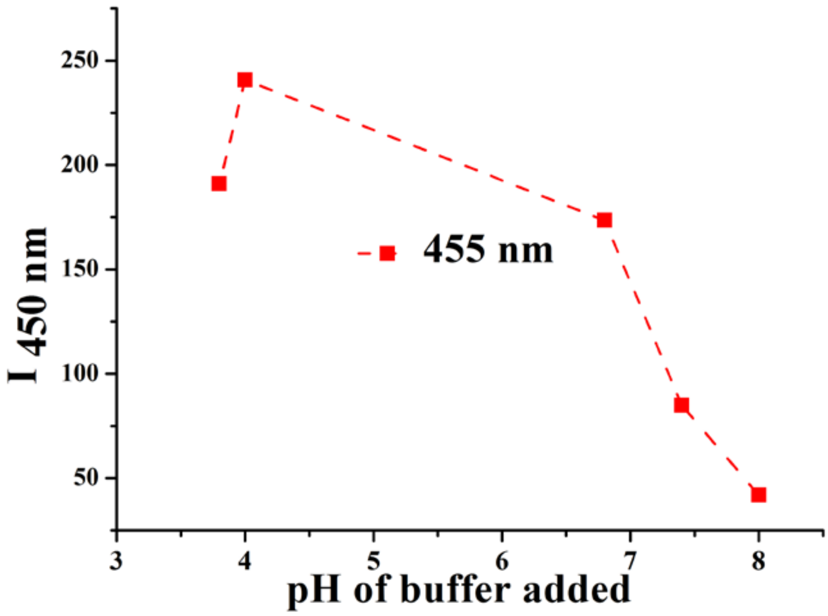

b)

Figure S9. Influence of medium acidity on the fluorescence intensity of **1** (5×10^{-5} M), measured in 90/10 (v/v) acetonitrile-citrate buffer (0.1 M SSC, pH = 3.8, 4.0, 6.8, 7.2, 8.0, before mixing with CH_3CN) mixed solution, λ_{ex} = 330 nm. a) λ_{em} = 400 nm; b) λ_{em} = 455 nm.

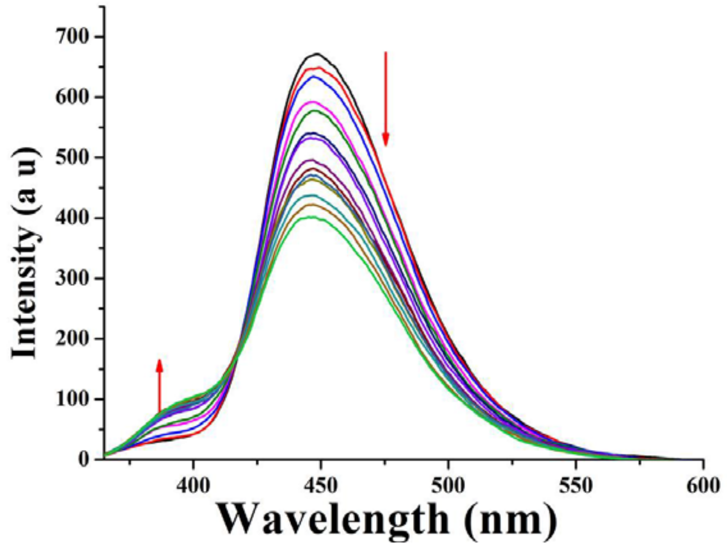

a)

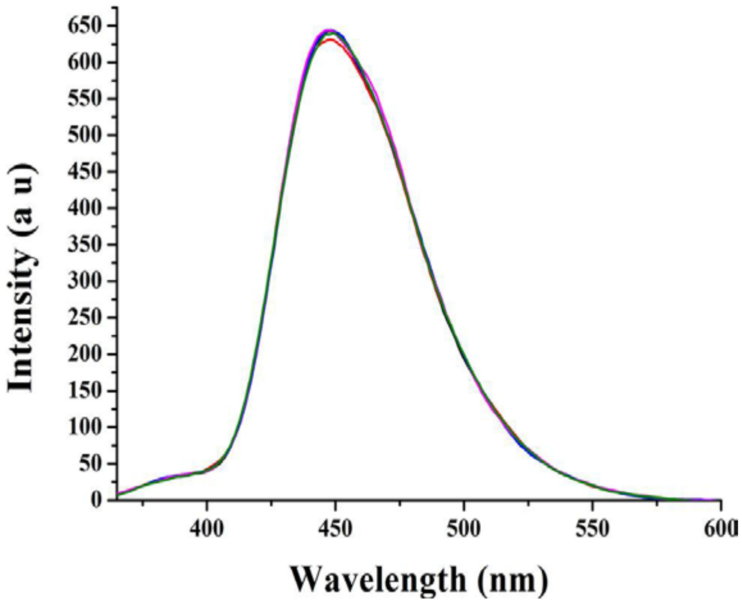

b)

Figure S10. a) Fluorescence titration of **1** (5×10^{-5} M) with addition of Zn^{2+} (from 0 to 50 equiv. Zn^{2+}) in buffer solution (CH_3CN/0.1 M SSC (pH 4.0, before mixing with CH_3CN) = 90/10, v/v); b) fluorescence (λ_{ex} = 330 nm) titration of **1** (5×10^{-5} M) with addition of F^{-} (as n-Bu_4N^+ salts, from 0 to 300 equiv. F^{-}) in buffer solution (CH_3CN/0.1 M SSC (pH 4.0, before mixing with CH_3CN) = 90/10, v/v), (λ_{ex} = 330 nm).

Table S1. Crystal data and structure refinement parameters of **1**-Zn^{2+}.

	1-Zn^{2+}
Chemical formula	$C_{68}H_{88}Zn_2N_8O_{30}$
Formula weight	1628.24
Crystal system	Triclinic
Space group	*P*-1
a/Å	9.6798(19)
b/Å	14.736(3)
c/Å	15.034(3)
α/°	69.35(3)
β/°	85.90(3)
γ/°	77.39(3)
V/Å^3	1958.3(7)
D_{calcd}/g cm^{-3}	1.381
Z	1
T	293(2)
μ/mm^{-1}	0.699
$R(int)$	0.1197
$R_1^a/wR_2^b[I>2\sigma(I)]$	0.1089/0.2276
GOF on F^2	1.090

^{a} $R = \Sigma(||F_0| - |F_C||)/\Sigma|F_0|$. ^{b} $Rw = [\Sigma w(|F_0|^2 - |F_C|^2)^2/(\Sigma w|F_0|^2)^2]^{1/2}$.

Table S2. Selected bond lengths (Å) and angles (°) for **1**-Zn[a]

Zn1—N3	1.971 (6)	Zn1—O7	1.973 (6)
Zn1—N1$^{\#1}$	1.967(6)	Zn1—O8$^{\#1}$	1.964 (6)
N3—Zn1—O8$^{\#1}$	111.3 (3)	N3—Zn1—O7	92.2 (3)
N3—Zn1—N1$^{\#1}$	127.7 (3)	O8$^{\#1}$—Zn1—O7	119.1 (3)
O8^{i}—Zn1—N1$^{\#1}$	93.8 (3)	N1$^{\#1}$—Zn1—O7	115.1 (3)

[a]Symmetry code: #1: -x+2, -y+1, -z.